Key Engineering Materials Vols. 257-258 (2004) pp. 95-100
online at http://www.scientific.net

Ductile Regime Machining of Single-Crystal CaF_2 for Aspherical Lenses

J. Yan [1], J. Tamaki [1], K. Syoji [2] and T. Kuriyagawa [2]

[1] Department of Mechanical Engineering, Kitami Institute of Technology
Koen-cho 165, Kitami, Hokkaido 090-8507, Japan

[2] Department of Mechatronics and Precision Engineering, Tohoku University
Aramaki-Aoba-01, Aoba-ku, Sendai 980-8579, Japan

Keywords: Ductile regime machining, Brittle material, Aspherical lens, Optics, Calcium fluoride, CaF_2, Diamond turning, Ultra-precision cutting

Abstract. Single-crystal calcium fluoride (CaF_2) is an important optical material used for dark-field imaging systems and short-wavelength photolithography systems. The fabrication of aspherical lenses using CaF_2 effectively eliminates the problems of color aberration and spherical aberration. The present paper describes a ductile regime machining system developed for fabricating aspherical surfaces on CaF_2 by single point diamond turning. In this system, the aspherical surface is enveloped by a straight-nosed diamond tool under three-axis simultaneous numerical control. The formation mechanism of the machining form error is analyzed and a rapid tool setting system is developed to aid the improvement of machining accuracy. The experimental results show that the system is effective for high-efficiency manufacturing of ultra-precision CaF_2 optics.

Introduction

Single-crystal CaF_2 is an optical material with high permeability over a wide wavelength range, from ultraviolet to infrared. It is used as lens substrate for applications such as dark-field imaging devices, home-use cameras and videos, microscopes, and photolithography systems. CaF_2 has unique optical properties including extremely low color aberration. This function is due to the abnormal partial dispersion characteristics of CaF_2, by which the degree of dispersion differs according to the light wavelength. For high-quality short wavelength optical systems, CaF_2 lenses are indispensable.

Up to date, most CaF_2 lenses are spherical lenses, which are finished by polishing. However, spherical lenses have the inherent problem of spherical aberration. Although spherical aberration can be avoided by a combination of multiple concave and convex lenses, in order to avoid spherical aberration using a single lens, the lens must be aspherical. The use of CaF_2 aspherical lenses solves the problems of both color aberration and spherical aberration simultaneously. Therefore, the development of the fabrication technology for CaF_2 aspherical lenses will contribute significantly to the improvement of imaging quality, miniaturization, and the production cost of optical products.

A potential method for machining CaF_2 aspherical optics would be single-point diamond turning (SPDT). SPDT is capable of ultra-precision machining of ductile materials such as nonferrous metals and plastics. However, CaF_2 is a highly brittle material and is extremely sensitive to temperature changes, leading to difficulties in machining. In a previous paper [1], one of the authors (J. Yan) carried out SPDT experiments on CaF_2 and found that thermal fracturing occurs during low tool feed wet cutting, which makes ductile machining difficult to achieve. To avoid thermal fracturing, two processing conditions were applicable: dry cutting and high tool feed wet cutting. Since dry cutting may cause rapid tool wear, the method of high tool feed wet cutting will be industrially beneficial. The latter requires that the tool feed rate must be sufficiently high while the undeformed chip thickness is kept extremely small. This paper presents an aspherical surface machining system that can satisfy these demands. The effectiveness of the system will be demonstrated through the fabrication of a CaF_2 aspherical lens.

Aspherical Surface Generation Method

As shown in Fig. 1, the topology of an aspherical surface can be expressed as the deviation from a sphere above the optic axis [2]. An axis-symmetric aspherical surface can be generally described by:

$$z(x) = \frac{Cx^2}{1 + \sqrt{1 - (k+1)C^2x^2}} + \sum_{i=1}^{m} a_i x^i \qquad (1)$$

Here, $C = 1/r$, where r is the radius of curvature of the sphere surface, x is the distance from the optic axis z, and k is the conic constant representing the eccentricity of the conic surface. For even i, a_i are aspherical deformation constants, and for odd i, a_i are aspherical coefficients used to define other polynomial curves by setting $C = 0$.

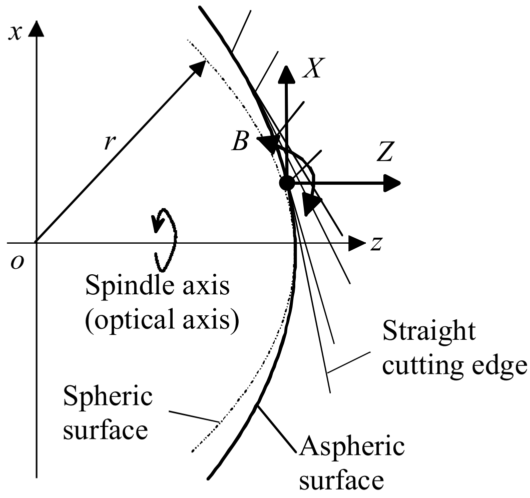

Fig. 1 Aspherical surface generation by the straight-line enveloping method.

Conventionally, an aspherical surface is cut using a round-nosed tool on a two-axis (X-Z) machine, where the arc of tool envelops the aspherical surface [3, 4]. In this case, undeformed chip thickness varies along the cutting edge. Thus, when machining brittle materials, a truly ductile response only occurs along the apex of the tool tip where the undeformed chip thickness is smaller than a critical depth d_c, while the upper material is fractured. For this reason, tool feed must be kept extremely small in order to obtain a crack-free surface [5, 6]. In the present work we used an alterative method, termed the straight-line enveloping method (SLEM), which has been used in silicon ductile machining [7, 8]. In this method, a nanometric level undeformed chip thickness can be obtained at a very large tool feed by using a straight-nosed diamond tool [9]. Ductile machining at a large tool feed improves both machining efficiency and tool life, also avoids thermal fracturing of CaF_2. On the other hand, as shown in Fig. 1, the use of a straight-nosed tool to cut an aspherical surface makes three-axis (X-Z-B) simultaneous control necessary. In the figure, the tool apex coincides with the center of the B-axis, which is perpendicular to the X-Z plane. A sufficiently small angle, namely cutting edge angle, is maintained between the cutting edge and the tangent line of the aspherical surface. When the tool moves along the X and Z axes while rotating about the B-axis, the straight cutting edge envelopes the aspherical surface.

In the conventional arc-enveloping method, tool geometry error and tool setting error are the two factors affecting the form error of product. Since the cutting point moves along the round edge during cutting, very high tool arc accuracy is required. In the straight-line enveloping method, the tool accuracy requirements are less strict because the cutting point is fixed on the tool. The only factor that causes form error in this method is tool setting error. Tool setting error is defined as the deviation of the actual tool position from the tool position specified in numerical control programs under initial conditions. One type of tool setting error is the de-centering error with respect to spindle axis center, which has been discussed in previous studies [3,4]. In this study, the use of the B-axis results in a new tool setting error: B-axis de-centering error (the deviation of the tool apex from the B-axis center).

Figure 2 (a) shows the formation mechanism of the machining form error due to B-axis de-centering error δ_{-z} (the tool apex deviates from the B-axis center in the $-z$ direction). For simplicity, we assume the ideal machining surface for numerical control to be a spherical surface S_0 with radius R. The path of the B-axis center will then be S_0', which has the same radius as S_0 but is described at a distance δ_{-z} from S_0. During cutting, as the B-axis rotates, the vector $\boldsymbol{\delta_{-z}}$ is always directed toward the

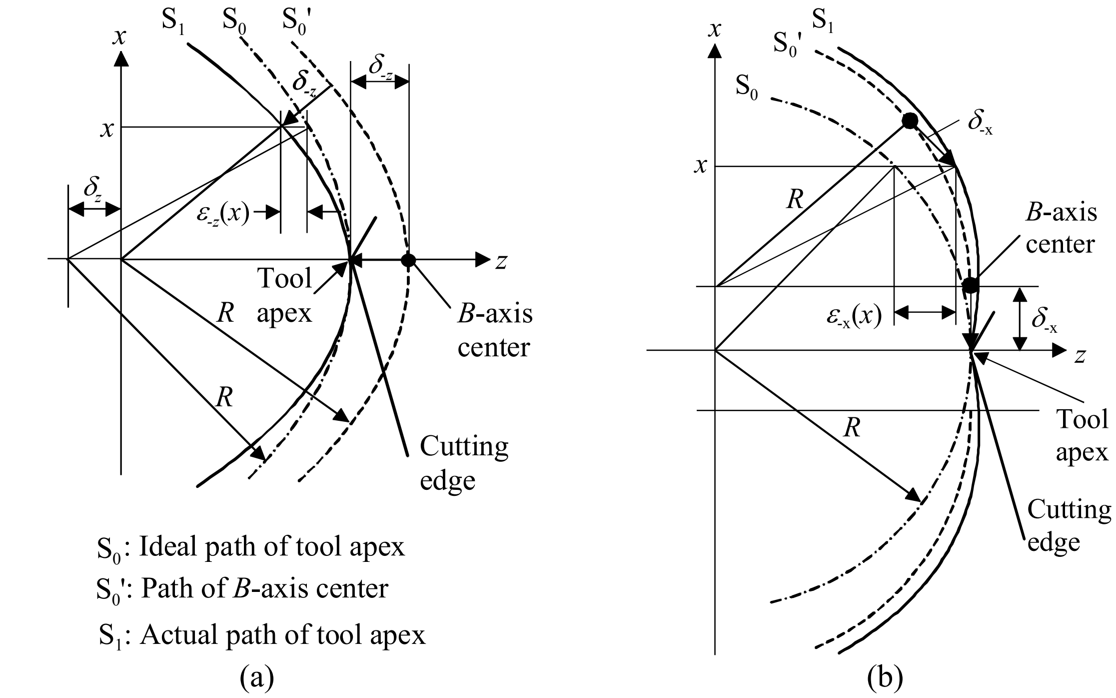

Fig. 2 Formation mechanism of the machining errors due to the tool de-centering error with respect to the *B*-axis. (a): de-centering in $-z$ direction, (b): de-centering in $-x$ direction.

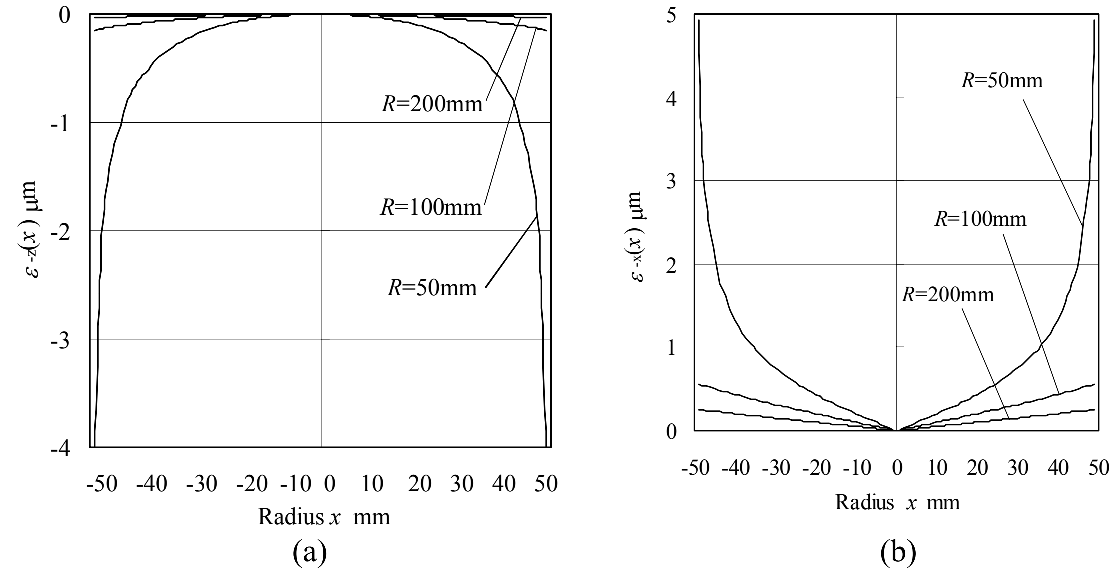

Fig. 3 Simulation results of the machining errors caused by the tool de-centering error with respect to the *B*-axis. (a): de-centering in $-z$ direction, (b): de-centering in $-x$ direction.

center of S_0'. Consequently, the actual tool path becomes S_1, a concentric circle of S_0'. The difference in the z coordinate between S_1 and S_0, $\varepsilon_{-z}(x)$, is the form error. Here, $\varepsilon_{-z}(x)$ can be calculated by

$$\varepsilon_{-z}(x) = \sqrt{(R-\delta_{-z})^2 - x^2} - \sqrt{R^2 - x^2} + \delta_{-z} \tag{2}$$

Similarly, when a *B*-axis de-centering error exists in the $-x$ direction (δ_{-x}) the formation mechanism of the form error is as shown in Fig. 2 (b). The ideal spherical surface, the path of the *B*-axis center, and the actual tool path, are indicated by S_0, S_0' and S_1, respectively, where the vector δ_{-x} is always directed toward the tangent of S_0'. In this case, the form error $\varepsilon_{-x}(x)$ can be calculated according to

$$\varepsilon_{-x}(x) = \sqrt{R^2 - x^2 + 2\delta_{-x} \cdot |x|} - \sqrt{R^2 - x^2} \quad (3)$$

The simulation results for the form error $\varepsilon_{-z}(x)$ and $\varepsilon_{-x}(x)$ are shown in Fig. 3 (a) and (b), respectively. Here, R is set to 50, 100 and 200 mm, and δ_{-z} and δ_{-x} are both set to 1 μm. In Fig. 3 (a), $\varepsilon_{-z}(x)$ is negative, indicating that the surface has been over-cut, whereas in Fig. 3 (b), $\varepsilon_{-x}(x)$ is positive, indicating that the surface has been under-cut. In both cases, the amplitude of the form error increases with x and decreases with R. Therefore, the form error will be significant when machining a small curvature surface, and the error increases with workpiece diameter. The trend of the variation of $\varepsilon_{-z}(x)$ is similar to $\varepsilon_{-x}(x)$; however, the amplitude of $\varepsilon_{-x}(x)$ is greater than that of $\varepsilon_{-z}(x)$ under otherwise identical conditions. The form errors resulting from B-axis de-centering error δ_{+z}, and δ_{+x}, and from multiple errors, can be calculated in the same way. The results showed that the form error $\varepsilon_{+z}(x)$ resulting from δ_{+z} is positive, indicating that the surface will be under-cut; whereas $\varepsilon_{+x}(x)$ resulting from δ_{x} is negative, indicating that the surface will be over-cut.

Experimental

Aspherical surface cutting experiments were carried out on an ultraprecision diamond turning machine, NACHI-ASP15. A photograph of the main section of the machine is shown in Fig. 4. This machine has an air bearing spindle, two perpendicular slide tables (X-axis and Z-axis) and a rotary table (B-axis). The X and Z tables are supported by high-stiffness hydrostatic bearings and are driven by AC servomotors via hydrostatic screws, allowing smooth nanometric movement with negligible mechanical friction. Laser hologram scales are used to accurately position the X and Z tables. The B-axis table is supported by hydrostatic bearings and driven by a friction drive in order to prevent from non-driven movement. Under numerical control, the X and Z tables can be moved at 10 nm per step and the B-table can be rotated with an angular resolution of 0.001˚. To isolate the machine from environmental vibration, the main section of the system was fixed to a granite bed, which is supported by air mounts.

In order to achieve the highest machining accuracy, the tool apex should be set at the center of the B-axis accurately. However, the B-axis center is not marked and direct measurement of the initial tool setting error is difficult. To solve this problem, a tool setting system was developed, allowing rapid setting of the tool to the B-axis center. A compact microscope and a CCD camera are used to observe the position of the tool on a PC monitor and to measure the tool de-centering error [7]. A three-dimensional tool post allows precise positioning of the tool. This method involves measuring the initial tool setting error and then finding the B-axis center using the numerical control system of

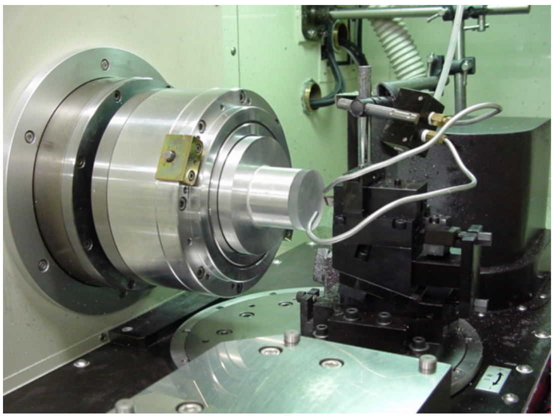

Fig. 4 Photograph of the main section of the *X-Z-B* three-axis aspherical generator.

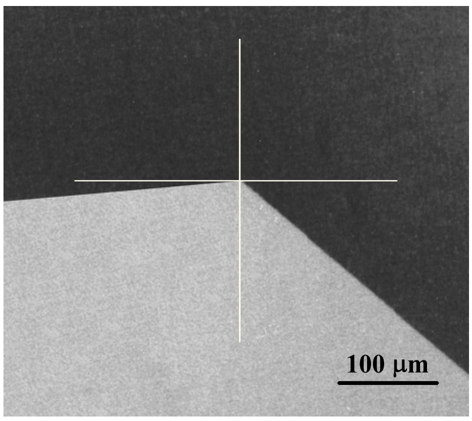

Fig. 5 Image of the straight-nosed diamond tool as observed by the tool setting system.

the machine itself. Using this technique, the *B*-axis de-centering error can be reduced to 1 µm level within several minutes. Figure 5 is an image of the straight-nosed diamond tool as observed by the tool setting system. The tool apex has been set to the *B*-axis center indicated by the cross.

An on-machine measurement system was developed to measure the machined aspherical surface and generate compensation data to achieve sub-micrometer level form accuracy. This system uses an air-bearing probe with a sapphire ball (radius 2 mm) fixed to the end. The probe scans the surface in the *X-Z* plane, and its displacement is detected using a laser hologram scale with a resolution of 10 nm. After machining, the aspherical surface is measured using the on-machine measurement system and an error data file is generated. If the form error is out of specification, the error data file is sent to the personal computer and the compensation data is calculated. The modified numerical control program is then transmitted back to the machine controller again for a compensation cut.

A single-crystal CaF_2 (111) substrate with dimensions of 50 mm diameter and 10 mm thickness was used in the experiments. The objective of the test cut was to generate a convex aspherical optical surface. The substrate was bonded to a diamond-turned aluminum blank using a 50˚C heat-softened glue and vacuum-chucked on the machine spindle. One face of the substrate was contoured from flat into the aspherical shape by rough cutting with a different diamond tool from that used for the finish cut. A new single-crystal diamond tool having a 1.8 mm long cutting edge and a 135˚ included angle was used for finish cut. The tool rake angle was –20˚, and the relief angle was 6˚. The –20˚ rake angle corresponds to the maximum ductile machining region in wet cutting [10].

Two finish cuts were performed; the first to remove subsurface damage resulting from the rough precuts, and the second as a compensation cut after on-machine measurement. The machining conditions for the first cut were as follows: depth of cut a = 10 µm, tool feed rate f = 10 µm/rev, and cutting edge angle κ = 0.8˚. The conditions for the second cut were a = 2 µm, f = 20 µm/rev and κ = 0.1˚. These conditions determine undeformed chip thickness h of 140 nm and 35 nm for the first and second cuts, respectively. The spindle rotation speed was set to 1500 rpm and kerosene mist was used as the cutting fluid.

Results

Figure 6 (a) shows a plot of form error measured by the on-machine measurement system after the first finish cut. The plots follow a triangular profile, the peak of which coincides with the center of the workpiece. The peak-to-valley amplitude of the form error is 1.166 µm. This profile indicates that the over-cut increases with the radius of cut. Thus, this form error can be attributed to the tool setting error δ_{-z} and/or δ_{+x}. Figure 6 (b) shows a plot of form error after the final compensation cut. The profile is relatively flat, with minor random variations. The peak-to-valley amplitude of the form error is only 0.107 µm, approximately 1/10 that of the first cut.

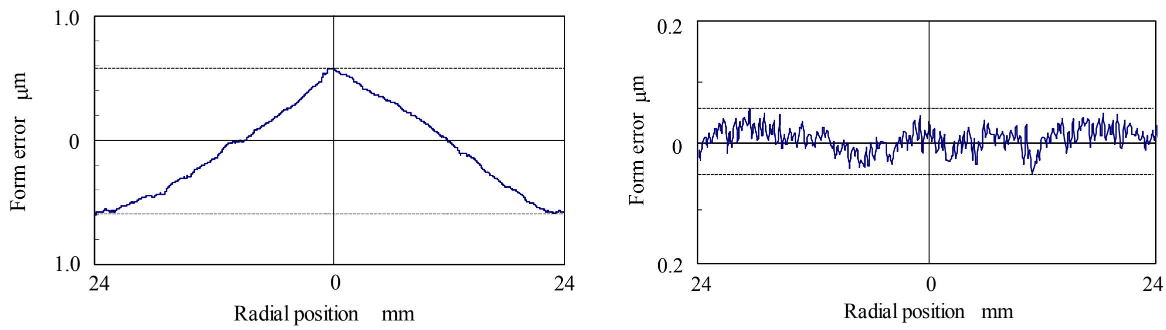

(a) (b)

Fig. 6 Form error distribution measured by an on-machine measurement system after (a) the first finish cut and (b) the final finish cut.

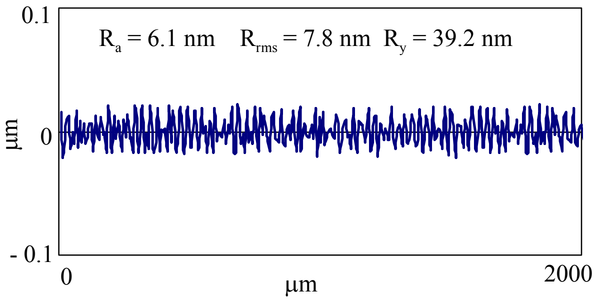

Fig. 7 Coross-sectional profile of the finished surface measured by non-contact measuring instrument.

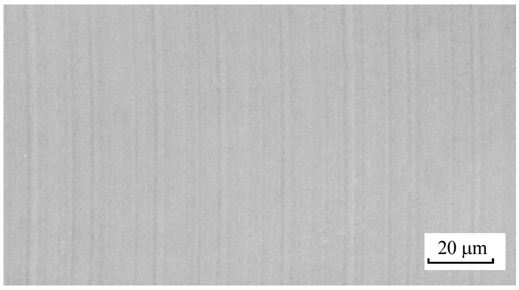

Fig. 8 Nomarski micrograph of the machined aspherical lens surface

The workpiece was then removed from the machine and the surface roughness was measured using a non-contact three-dimensional surface measurement instrument (Mitaka NH-3SP). Figure 7 shows the measurement result. The surface roughness is 6.1 nm R_a, 7.8 nm R_{rms} and 39.2 nm R_y. Figure 8 is a Nomarski micrograph of the produced CaF_2 aspherical lens. The lens surface is completely ductile-regime machined without micro-fractures. The two finish cuts for this lens required approximately 3 minutes, demonstrating a very high machining efficiency of the proposed method.

Summary

A system for fabricating aspherical surfaces on single-crystal CaF_2 by diamond turning was described. This system involves using a straight-nosed tool under *X-Z-B* 3-axis simultaneous control, and enables high tool feed ductile-regime cutting. The formation mechanism of the machining form error due to the tool de-centering error with respect to the *B*-axis center was analyzed. A tool setting system and an on-machine measurement system were developed in order to improve machining accuracy. An aspherical lens with form accuracy of 0.107 μm and surface roughness of 39.2 nm R_y was produced at a high tool feed rate of 20 μm/rev. The results illustrate that the system is effective for the high-efficiency and high-accuracy fabrication of CaF_2 aspherical optics.

Acknowledgements

J. Yan and K. Syoji acknowledge the grants from the Japan New Energy and Industrial Technology Development Organization (NEDO), project number 01A38004, and from the Ministry of Education, Science, Sports and Culture, Grant-in-Aid for Young Scientists, project number 15760073.

References

[1] J. Yan, K. Syoji, T. Kuriyagawa, K. Tanaka and H. Suzuki: *Proc. of the ASPE*, 22, (2000) 66.
[2] D. C. O'Shea, Wiley, New York, 1985.
[3] H. Suzuki, T. Kitajima and S. Okuyama: *J. Jap. Soc. Prec. Eng.*, Vol.65, 3, (1999) 401.
[4] W. B. Lee, C. F. Cheung, W. M. Chiu and T. P. Leung: *J. Mater. Proc. Tech.*, Vol.99 (2000) 129.
[5] W.S. Blackly and R.O. Scattergood: *Prec. Eng.*, Vol.13, 2 (1991) 95.
[6] T. Nakasuji, S. Kodera, S. Hara, H. Matsunaga, N. Ikawa and S. Shimada: *Ann. CIRP*, Vol.39, 1 (1990) 89.
[7] J. Yan, K. Syoji and T. Kuriyagawa: *J. Jap. Soc. Prec. Eng.*, Vol.68, 4, (2002) 561.
[8] J. Yan, J. Tamaki, K. Syoji and T. Kuriyagawa: *Key Eng. Mater.*, Vol. 238-239 (2003) 43.
[9] J. Yan, K. Syoji, T. Kuriyagawa and H. Suzuki: *J. Mater. Proc. Tech.*, Vol. 121 (2002), 363.
[10] J. Yan, J. Tamaki, K. Syoji and T. Kuriyagawa: *Int. J. Adv. Manuf. Tech.*, in press.